International Journal of Pharmaceutics 423 (2012) 516–524

Contents lists available at SciVerse ScienceDirect

International Journal of Pharmaceutics

journal homepage: www.elsevier.com/locate/ijpharm

Pharmaceutical Nanotechnology

Biodegradable nanoparticles mimicking platelet binding as a targeted and controlled drug delivery system

Soujanya Kona[a,b], Jing-Fei Dong[c], Yaling Liu[d,e], Jifu Tan[d], Kytai T. Nguyen[a,b,*]

[a] Department of Bioengineering, University of Texas at Arlington, TX, United States
[b] Biomedical Program, University of Texas Southwestern Medical Center, Dallas, TX, United States
[c] Department of Medicine, Baylor College of Medicine, Houston, TX, United States
[d] Department of Mechanical Engineering and Mechanics, Lehigh University, Bethlehem, PA, United States
[e] Bioengineering Program, Lehigh University, Bethlehem, PA, United States

ARTICLE INFO

Article history:
Received 13 September 2011
Received in revised form 9 November 2011
Accepted 28 November 2011
Available online 6 December 2011

Keywords:
Biodegradable nanoparticles
Endothelial cells
Platelets
Glycoprotein Ib
Parallel plate flow system

ABSTRACT

This research aims to develop targeted nanoparticles as drug carriers to the injured arterial wall under fluid shear stress by mimicking the natural binding ability of platelets via interactions of glycoprotein Ib-alpha (GPIbα) of platelets with P-selectin of damaged endothelial cells (ECs) and/or with von Willebrand factor (vWF) of the subendothelium. Drug-loaded poly(D,L-lactic-co-glycolic acid) (PLGA) nanoparticles were formulated using a standard emulsion method and conjugated with glycocalicin, the external fraction of platelet GPIbα, via carbodiimide chemistry. Surface-coated and cellular uptake studies in ECs showed that conjugation of PLGA nanoparticles, with GPIb, significantly increased nanoparticle adhesion to P-selectin- and vWF-coated surfaces as well as nanoparticle uptake by activated ECs under fluid shear stresses. In addition, effects of nanoparticle size and shear stress on adhesion efficiency were characterized through parallel flow chamber studies. The observed decrease in bound nanoparticle density with increased particle sizes and shear stresses is also explained through a computational model. Our results demonstrate that the GPIb-conjugated PLGA nanoparticles can be used as a targeted and controlled drug delivery system under flow conditions at the site of vascular injury.

1. Introduction

Recent research has focused on developing nanoparticle (NP) delivery systems for drug and gene therapy to treat various cardiovascular pathological conditions (Davda and Labhasetwar, 2002; Eniola and Hammer, 2005b; Zou et al., 2005). Upon injury or under conditions like thrombosis (the formation of a blood clot), inflammation, and restenosis (the narrowing of a blood vessel), the endothelium is activated and shows an increased expression of endothelial cell adhesion molecules, like P-selectin and E-selectin, compared with normal, healthy cells (Eniola and Hammer, 2005b; Lutters et al., 2004; Sakhalkar et al., 2003; Zou et al., 2005). Specific ligand and antibodies bound to these molecules have been used for targeting therapeutic agents to the damaged endothelium. For example, E-selectin immunoliposomes loaded with the doxorubicin significantly decreased cell survival in activated ECs, but had no effect on inactivated ECs (Spragg et al., 1997). In addition, sialyl Lewis^x (sLe^x)-conjugated microparticles were shown to effectively roll on surfaces coated with purified P-selectin, similar to the rolling of leukocytes on P-selectin surfaces (Eniola and Hammer, 2005a,b). Conjugation of recombinant P-selectin glycoprotein ligand-1 (PSGL-1) to micro- or nano-particles also showed the selective adhesion of these particles to cytokine-activated endothelium *in vitro* and in animal models (Sakhalkar et al., 2003, 2005). However, a major limitation of NP delivery to the cardiovascular system is the inefficient arrest of the NPs to the vascular wall under blood flow (Blackwell et al., 2001; Lin et al., 2010).

Herein, we present a novel drug delivery system that mimics platelets binding to the injured vessel wall under physiological flow conditions. We chose glycoprotein Ib (GPIb) as the targeting ligand, because its role in platelet adhesion to the vascular wall under high shear flow conditions is well-recognized (Dong et al., 2000; Kumar et al., 2003). GPIb also serves as the targeting ligand that binds to both P-selectin that is highly expressed on damaged endothelium and von Willebrand factor (vWF), which is deposited on the luminal surface at the arterial injured site within a few minutes of injury via balloon angioplasty (Andre et al., 1997; Giddings et al., 1997). Our hypothesis is that these unique "platelet-mimicking nanoparticles" would exclusively attach to the damaged arterial wall under high shear stress conditions, increasing cellular retention and uptake of NPs.

* Corresponding author at: University of Texas at Arlington, Department of Bioengineering, 500 UTA Blvd, ERB-241, Arlington, TX 76010, United States.
Tel.: +1 817 272 2540; fax: +1 817 272 2251.
E-mail address: knguyen@uta.edu (K.T. Nguyen).

0378-5173/$ – see front matter © 2011 Elsevier B.V. All rights reserved.
doi:10.1016/j.ijpharm.2011.11.043

In this study, we formulated and characterized dexamethasone-loaded, biodegradable poly(D,L-lactide-co-glycolide) (PLGA) nanoparticles. We chose dexamethasone (DEX), an immune suppressant, as the model drug, because it has been shown to reduce the development of intimal hyperplasia (Petrik et al., 1998) and exhibit both anti-inflammation effects on ECs and anti-migration and anti-proliferation effects on SMCs (Park and Yoo, 2006; Van Put et al., 1995). Cellular uptake of the control and GPIb-conjugated NPs was detected in human aortic endothelial cells (HAECs) by fluorescent measurements and confocal microscopy imaging. Furthermore, GPIb-conjugated NPs were also investigated for their effectiveness in adhering onto P-selectin- and vWF-coated surfaces and for their cellular uptake by HAECs under physiological flow conditions using a parallel flow chamber system. The ability of the GPIb-conjugated NPs to adhere to the injured rat artery was also preliminarily studied via an *ex vivo* arterial model.

2. Methods

2.1. Materials

Poly(D,L-lactic-co-glycolic acid) (PLGA) (inherent viscosity – 0.15–0.25 dl/g, copolymer ratio 50:50) with carboxyl end groups was purchased from Lakeshore Biomaterials (Birmingham, AL). Chemicals, if not specified, were purchased from Sigma–Aldrich (St. Louis, MO). HAECs, low serum growth supplement (LSGS consisting of 2% fetal bovine serum, hydrocortisone (1 μg/ml), human epidermal growth factor (10 ng/ml), basic fibroblast growth factor (3 ng/ml), and heparin (10 μg/ml)), as well as cell culture medium, supplements, and buffers, including trypsin–EDTA, Medium 199 (M199), fetal bovine serum (FBS), and penicillin–streptomycin were procured from Invitrogen Corporation (Carlsbad, CA). Glycocalicin was purified from platelet lysates, as previously described (Romo et al., 1999).

2.2. Formulation of NPs

PLGA NPs were formulated using the double emulsion-solvent evaporation method since the water soluble form of dexamethasone (dexamethasone–cyclodextrin complex from Sigma) was used. In brief, dexamethasone (DEX) solution (30 mg of DEX in 300 μl of distilled water) was emulsified in an organic chloroform dye-polymer solution (0.05 mg 6-courmarin, which is used as a fluorescent marker for visualization and quantification of PLGA nanoparticles, and 90 mg PLGA polymer in 3 ml chloroform) using a probe sonicator (Misonix Inc., 3000, Farmingdale, NY) at 33 W energy output for 30 s to form the primary water/oil emulsion. The primary emulsion was further emulsified into an aqueous solution of polyvinyl alcohol (PVA) (0.6 g of PVA in 12 ml distilled water) by sonication, and the secondary (w/o/w) emulsion was then stirred overnight at room temperature to allow for any residual solvent to be evaporated. NPs were then ultra-centrifuged at 30,000 rpm (Beckman Coulter Inc., Fullerton, CA) to remove un-reacted materials, including PVA and non-entrapped drugs. The recovered NPs were then collected by ultracentrifugation, resuspended in distilled water, and lyophilized. In a similar manner, NPs without DEX and 6-coumarin dyes as well as NPs with the sizes of 500 nm (using 1%, w/v, PVA) and 1 μm (using 0.5%, w/v, PVA) were formulated using the same method. Nanoparticles without drug and dye were used for biocompatibility studies, and all other studies used drug-loaded nanoparticles, if not specified.

2.3. Characterization of PLGA NPs

The formulated NPs were characterized for their morphology, particle size, polydispersity and surface charge (zeta potential) using transmission electron microscopy (TEM, JEOL 1200 EX Electron Microscope) and ZetaPALS dynamic light scattering (DLS) detector (Brookhaven Instruments, Holtsville, NY) at room temperature.

2.4. Determination of drug entrapment efficiency and drug release studies

To directly determine the percentage of drugs entrapped in the NPs, the freeze-dried particles were dissolved in a mixture of $CHCl_3$ and DI water, which allowed the encapsulated drugs to be released from PLGA NPs into the aqueous phase. The drug amount was then experimentally measured and compared to the total amount of DEX used in the nanoparticle formulation.

For *in vitro* drug release studies, stock suspensions of drug-loaded nanoparticles were prepared in 0.1 M PBS. The NP suspension was placed inside spectrum dialysis bags (the molecular weight of dexamethasone is 392.5 Da) and dialyzed against PBS at 37 °C for 21 days on a shaker to allow the released drugs to be diffused into the dialysates. At different intervals, 1 ml of dialysate was collected from each sample and replaced with 1 ml of fresh PBS. The collected dialysate was stored at −20 °C for later analysis. To determine the amount of drugs released, absorbance of the samples was read at 242 nm. The amount of released drugs was determined by a standard DEX curve and correlated to the loading amount to determine the cumulative percent drug release.

2.5. Conjugation of PLGA nanoparticles with glycocalicin

The formulated PLGA NPs were conjugated with glycocalicin, the external fraction of platelet GPIbα (MW-145 kDa), using carbodiimide chemistry and avidin–biotin affinity, as described in our previous work with polystyrene nanoparticles consisting of the carboxylated end groups (Lin et al., 2010). In brief, glycocalcin was biotinylated using the Biotin-X-NHS Kit (EMD Biosciences Inc., San Diego, CA) following the manufacturer's instructions. In parallel, PLGA nanoparticles (40 mg) were added to 4 ml of a 15 mg/ml EDC solution in 0.1 M MES buffer (pH 4.75) and incubated at room temperature for five hours to ensure activation of the carboxyl groups on PLGA nanoparticles. After 5 h, 500 μg of avidin (EMD Biosciences Inc.) was added to the nanoparticle suspension and allowed to react with the activated carboxyl groups overnight against 0.1 M sodium bicarbonate solution (pH 8.5). The avidin-conjugated PLGA nanoparticles were washed to remove non-reacted materials via dialysis and recovered by freeze-drying. After washing to remove non-reacted materials via dialysis, the biotinylated glycocalicin prepared earlier was added and incubated with avidin-conjugated PLGA NPs at room temperature under gentle agitation for two hours and then purified by dialysis followed by ultracentrifugation to remove non-reacted materials. These conjugated NPs were then characterized by TEM and DLS. Avidin and biotin affinity was used to enhance the functional groups for peptide conjugation as one avidin would react with four biotinylated molecules. To confirm the conjugation of glycocalcin onto nanoparticles, 100 μl of 30 μg/ml primary mouse monoclonal antibodies against glycocalcin was added to GPIb-conjugated nanoparticles in PBS. A fluorescent (red) secondary antibody was added to the nanoparticle suspension and incubated for one hour. After washing, nanoparticles were observed and analyzed using the enhanced optical Cytoviva microscope.

2.6. In vitro stability of nanoparticles

We performed *in vitro* studies of long-term stability and protein binding on our NPs. Since PLGA nanoparticles would be degraded over time, we only studied the particle stability to determine whether particles would be aggregated in the saline and serum

conditions for up to 5 days. Either control or GPIb-conjugated nanoparticle samples ($n = 4$) were suspended in PBS buffer and incubated at 37 °C for 5 days to determine their stability in PBS. The size of the NPs was measured every 24 h using DLS. Stability and protein binding of the nanoparticles in the serum were carried out by suspending GPIb-conjugated NPs and control NPs in 100% FBS for 5 days at 37 °C. Size measurements were done every 24 h by DLS for up to 5 days.

2.7. Culture of human aortic endothelial cells (HAECs)

HAECs were cultured in M199 supplemented with 10% FBS, 1% penicillin–streptomycin and LSGS. Upon confluence, cells up to passage 10 were used for the experiments. Since prior research has shown that the use of high serum (greater than 1%) medium increases the rate of endocytosis and exocytosis of PLGA NPs (Chithrani and Chan, 2007; Panyam and Labhasetwar, 2003), we used low serum (1% serum) M199 for all the cellular studies.

2.8. Preparation of P-selectin and vWF coated slides and activated HAECs

Culture dishes were incubated with either 20 μg/ml P-selectin (R&D Systems) or 5 μg/ml vWF (Calbiochem) solution overnight at 4 °C. This was followed by a 1-h incubation with 1% (w/v) BSA solution to block nonspecific binding and washing with PBS. To prepare activated HAECs, cells were seeded on pre-etched glass slides at 10^4 cells/cm^2 and treated with 25 mM histamine for 12 min. Both coated surfaces and histamine-treated cells were used immediately for the experiments.

2.9. Cellular studies of PLGA NPs by HAECs

To determine the biocompatibility of the NPs on HAECs, we incubated HAECs with various concentrations (0–1000 μg/ml) of control and GPIb-conjugated NPs without any drug loading for up to 24 h, and cell viability was then assessed using MTS assays (Promega Corp.) following the manufacturer's instructions.

To determine cellular uptake of NPs, HAECs were seeded in 48-well plates at 10^4 cells/cm^2 and allowed to grow for 2 days before cells were quiescent. The dose-dependent and time-dependent cellular uptake of control and GPIb-conjugated NPs by HAECs were investigated. For dose studies, HAECs were incubated with the respective NP suspensions (0–500 μg/ml) prepared in low serum growth medium for 1 h. For the time-dependent NP uptake study, HAECs were incubated with 100 μg/ml of control and GPIb-conjugated NP suspensions for varying periods of time (0–6 h).

To examine the effects of shear stress on the uptake of NPs by HAECs, we seeded HAECs on pre-etched glass slides at a density of 10^4 cells/cm^2 and allowed them to reach 80% confluence. The HAECs were then exposed to medium containing NPs (200 μg/ml) at varying shear stresses (0–20 dyn/cm^2) for 30 min using the parallel plate flow chamber system, as described previously (Nguyen et al., 2001). We chose the parallel plate flow chamber due to its ability to generate constant levels of shear stress. Cells in static conditions served as the controls.

After the experiments, cells were washed 3 times with cold PBS to remove any adhering NPs and then lysed by incubating with 1% Triton® X-100 for 1 h. This cell lysate was used to determine the total cell protein, which corresponds to the cell number, using Pierce BCA protein assays (Fisher Scientific, Hampton, NH) following the manufacturer's instructions, and a standard curve was generated using the known number of cells. In order to quantify NP uptake by HAECs, the fluorescent intensity of NPs in cell lysates, as well as the NP standards, was measured at EX 480 nm/EM 510 nm using a microplate reader (Infinite M200, Tecan USA Inc.). NP uptake was calculated by normalizing particle concentration with the cell number of each sample. The observed optimal time and dose where the cellular uptake was saturated from these studies were used for all further studies.

2.10. Adhesion and cellular uptake of GPIb-conjugated NPs under flow conditions

Coated culture dishes (either with P-selectin or with vWF) were assembled in a parallel flow circular chamber (GlycoTech, Gaithersburg, MD) for surface studies, while glass slides with activated monolayer HAECs for cell studies were assembled into the parallel flow plate chamber for cellular studies. To minimize the cost and the amount of protein required for coating, we used the parallel flow circular chamber for coated surface studies (Brown and Larson, 2001). For cellular studies, we used the parallel flow plate chamber to get enough cells for the bioassays' analyses. Both parallel flow chamber systems have been well-characterized and demonstrated to generate the shear stress levels similar to those of *in vivo* conditions (Brown and Larson, 2001; Nguyen et al., 2001). We compared the adhesion of different-sized conjugated particles (200–1000 nm) to P-selectin- and vWF-coated surfaces under varying shear stresses (0–25 dyn/cm^2). In addition, we performed a comparative non-cellular flow study, where the flow chamber was set to produce 15 dyn/cm^2 of shear stress, as this shear stress level is presented as the average arterial flow condition (Nguyen et al., 2001). Three groups of NPs were used, namely control NPs, GPIb-conjugated NPs and anti-GPIb-conjugated NPs (GPIb-conjugated NPs with their binding sites blocked by anti-GPIb antibodies). After the flow studies, the amount of NPs bound to the coated surface was measured by a spectrofluorometer.

We also performed comparative cellular uptake studies of control NPs and GPIb-conjugated PLGA NPs under static and flow conditions to evaluate the effectiveness of our GPIb-conjugated NPs. To study the adhesion and uptake efficacy of our conjugated NPs to activated HAEC cells under flow conditions, activated HAECs on glass slides were exposed with either non-conjugated (control) or GPIb-conjugated NP suspensions (100 μg/ml) under varying levels of shear stress (0–25 dyn/cm^2). Samples in the static condition were also studied for comparison. Following the flow experiments, cells were washed with PBS, lysed and analyzed for the cellular uptake of NPs as described earlier. For confocal imaging, after the completion of experiments, cells were washed with cold PBS, followed by the addition of cold FM® 4-64 FX (5 μg/ml, Molecular Probes, Invitrogen, Eugene, OR) in PBS for 5 min to stain cell membranes. HAECs were fixed with paraformaldehyde and imaged using a confocal laser scanning microscope (Leica) equipped with FITC (EX (λ) 488 nm, EM (λ) 515 nm) and TRIC filters (EX (λ) 561 nm, EM (λ) 635 nm). Slice thickness was set at 0.1 μm, with 32 slices taken per image. Images were processed by ImageJ software (NIH, ImageJ 1.40).

2.11. Simulation studies on nanoparticle binding

To interpret the experimental results, we used a computational model to study the effects of flow shear rate and particle size on adhesion properties and validated our model with the experimental data. The steady state probability of adhesion P_a can be characterized by probabilistic kinetic formulation of McQuarrie (Riper et al., 1998) and Decuzzi (Decuzzi and Ferrari, 2006) since the ligand–receptor binding process is stochastic in nature:

$$P_a = m_r m_l K_a^o A_c \exp\left[-\frac{\lambda F_{dis}}{k_B T m_r A_c}\right] \quad (1)$$

where m_r is surface density of receptors, m_l is ligand density on particle surface, A_c is the contact area of particle, $k_B T$ is thermal energy

of the system, and K_a^o is the affinity constant of the ligand–receptor pair at zero load. F_{dis} is the dislodging force due to hydrodynamic forces, which is comprised of drag force along the flow direction F and torque T.

Hydrodynamic forces f are experienced on the particles and can be expressed as

$$f = \frac{F_{dis}}{A_c} = \frac{F}{A_c} + \frac{2T}{A_c r_0} \quad (2)$$

where F_{dis} is the dislodging force due to fluid flow, A_c is the contact surface area of the particle, r_o is the critical radius of the particle, T is the torque (component of the dislodging force) and F is the drag force component of the dislodging force along the direction of the flow. It is evident from Eq. (2) that the force is a function of the surface area of contact and particle size. Force and Torque are functions of the local fluid velocity (Decuzzi and Ferrari, 2006) defined by

$$F = 6\pi a l \mu S F^s \quad (3)$$

and

$$T = 4\pi a^3 \mu S T^s \quad (4)$$

where a is the characteristic size of the particle, μS is the shear stress at the wall, l is the distance between the center of the particle to the substrate wall. F^S and T^S are the coefficients of drag and torque, which are functions of the spherical particle radius r. Hence, dislodging force and particle size are determinant factors in particle adhesion probability. The density of adhered particles under different shear stress rates is calculated from the coupled continuum convection–diffusion–reaction simulation, incorporated with particulate adhesion probability and compared with the experimental data.

2.12. Preliminary ex vivo retention study of GPIb-conjugated NPs

All animal experiments were performed in accordance with the animal welfare policies and IACUC-approved protocols of the University of Texas at Arlington. For the NP retention study, the NPs were loaded with NIR-797 (Sigma–Aldrich, St. Louis, MO) fluorescent dyes and conjugated with GPIb peptides as described above. Carotid balloon injury was induced in six male Sprague–Dawley rats after giving general anesthesia intraperitoneally. Then, through a midline neck incision, the common, external, and internal carotid arteries were exposed by blunt dissection, followed by the introduction of a 2F Fogarty balloon catheter into the external carotid artery via an arteriotomy which advanced to the origin of the left common carotid artery. The balloon was then gradually inflated to 7 atm to cause a balloon injury and then deflated. This process was repeated 3 times to consistently produce the injury along the length of the common carotid artery similar to a standard angioplasty procedure. After removal of the balloon catheter, the injured artery was infused with either control NPs or GPIb-conjugated NPs (5 mg/ml) over 3 min. When the NPs were delivered, the apical end was also clamped with a vascular clamp. This created a closed loop system that allowed the contact of the NPs with the injured vessel wall for a short time, after which the vascular clamps were removed to restore the blood circulation in the injured artery. After 30 min, the arteries were then collected and extensively washed with PBS over 3 min to remove non-adherence nanoparticles, excised, and imaged using the KODAK FX Pro imaging system (Carestream, EX-760 nm/EM-830 nm).

2.13. Statistical analysis

Results were analyzed using one-way ANOVA and t-tests with $p < 0.05$ (StatView 5.0 software, SAS Institute). *Post hoc* comparisons were made using the Fisher's least significant differences (LSD). All of the results are given as mean ± SD (n = 3–6 experiments).

3. Results

3.1. Characterization and in vitro stability of drug-loaded PLGA NPs and drug-loaded, GPIb-conjugated PLGA NPs

The mean hydrodynamic diameter of the drug-loaded PLGA NPs as determined by ZetaPALS was 180 ± 47 nm, while the drug-loaded, GPIb-conjugated PLGA NPs showed a size of 220 ± 4735 nm. The surface charge of the drug-loaded PLGA NPs was −32 ± 470.8 mV, while the drug-loaded, GPIb-conjugated PLGA NPs showed a zeta potential of −13 ± 470.5 mV. TEM images (Fig. 1A) demonstrated the spherical morphology and range size of the drug-loaded, GPIb-conjugated NPs within 100–250 nm. Conjugation of GPIb onto PLGA NPs was also confirmed through observation of antibodies against GPIb (red) on PLGA NPs using the enhanced optical fluorescent microscope, Cytoviva microscope (results not shown).

For stability studies of non-conjugated and GPIb-conjugated PLGA nanoparticles, size measurements of both NPs via DLS in PBS demonstrated that the NPs' size was comparable over the five-day period without any significant change in particle size (results not shown). In addition, the protein binding and long-term stability of the control NPs and GPIb-conjugated NPs in FBS showed that the NPs did not aggregate and maintained their size over the studied time period after an initial 10–20 nm increase in size (results not shown).

3.2. Drug release profile from drug-loaded GPIb-NPs

To determine the efficacy of drug-loaded NPs as a sustained drug delivery carrier, we performed an *in vitro* drug release study to measure the amount of DEX released from the NPs over a course of time. The loading efficiency of DEX into the PLGA NPs was calculated to be about 66%. Release kinetics of DEX from PLGA NPs indicated a sustained drug release from the NPs showing the ability for a continued drug release for up to 3 weeks with about 80% of loaded drugs released at a period of 3 weeks (Fig. 1B).

3.3. Cellular studies of NPs by HAECs

The cellular viability results show that both groups of NPs (PLGA NPs and GPIb-conjugated NPs without any drug loading) exhibited greater than 90% cell viability after HAECs were exposed to NPs at concentrations of up to 500 μg/ml for 24 h (Fig. 1C). However, at a concentration of 1000 μg/ml, cells exposed to control NPs displayed only around 70% viability, while cells exposed to GPIb-conjugated NPs still showed more than 90% cell viability. NP cellular uptake studies indicated the uptake of nanoparticles by HAECs to be both dose- and incubation time-dependent. HAEC cellular uptake for both groups of NPs saturated at concentrations of 300 μg/ml (Fig. 2), while after 4 h of incubation, the uptake reached a plateau (results not shown). In addition, the GPIb-conjugated NPs exhibited a fivefold higher uptake by HAECs, compared to the control NPs.

3.4. GPIb-conjugated NPs improved adhesion on coated surfaces and cellular uptake by HAECs under physiological flow conditions

We examined the adhesion of different-sized GPIb-conjugated NPs on vWF- and P-selectin-coated surfaces under different flow rates. The number of NPs that adhered to vWF surfaces reduced with increasing shear stress; however, 200 nm-sized NPs adhered in greatest numbers on vWF-coated surfaces compared to 500 nm- and 1 μm-sized particles (dots in Fig. 3 for experimental results).

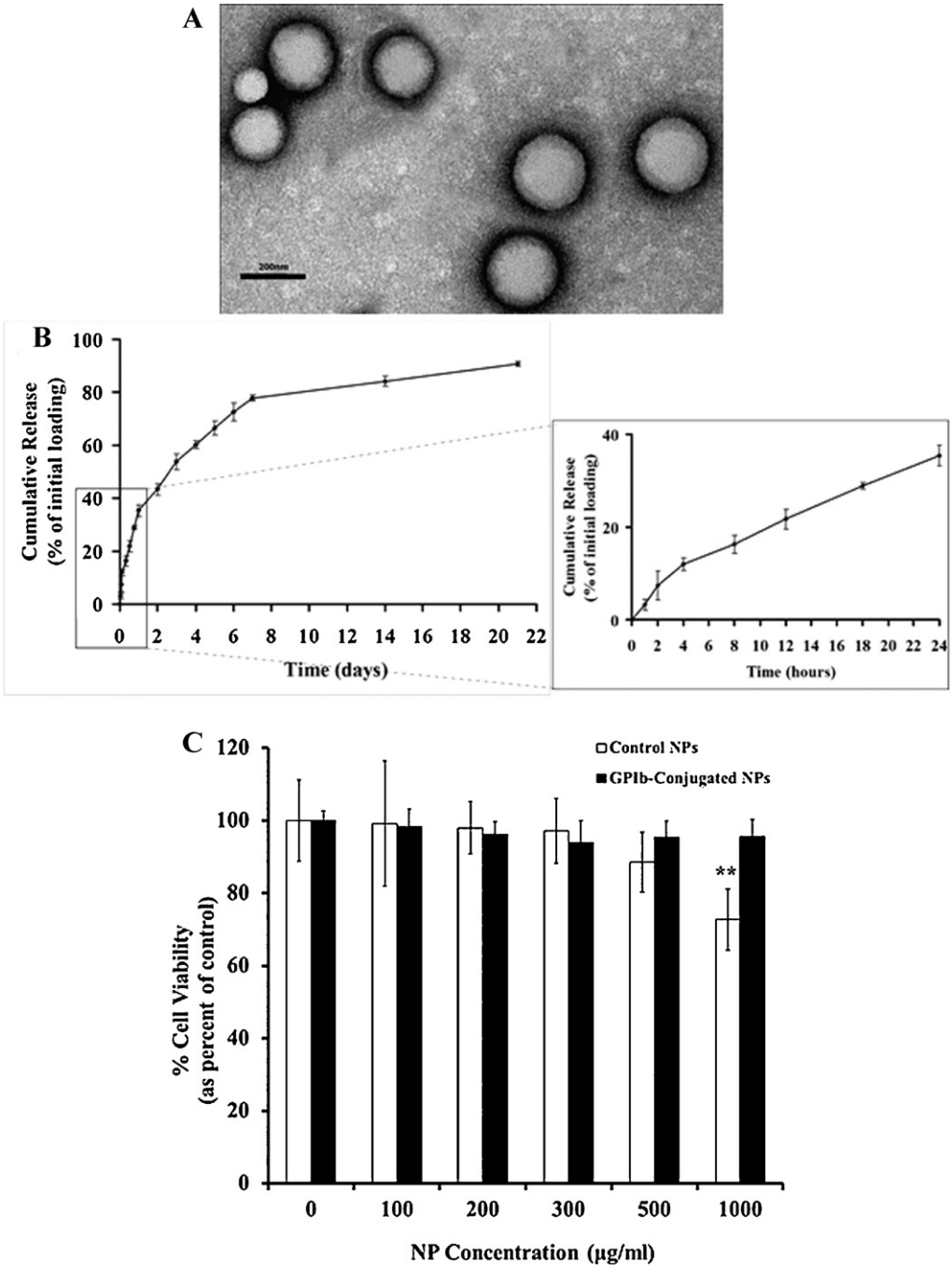

Fig. 1. Characterization of drug-loaded, GPIb-conjugated PLGA NPs. (A) Representative transmission electron microscopy (TEM) images of drug-loaded, GPIb-conjugated PLGA NPs. Scale bar – 200 nm. (B) *In vitro* release profile of Dexamethasone from the drug-loaded PLGA NPs at 37 °C. Inset is the cumulative percentage release of DEX over 24 h. Values represent mean ± standard deviation ($n = 4$). (C) Biocompatibility of control NPs and GPIb-conjugated NPs without any drug loading. Cells were exposed to respective nanoparticle suspensions for 24 h, and cell viability was determined via MTS assays. Cells not exposed to nanoparticles served as controls (100% cell viability). ** Indicates significant differences compared to the control samples ($p < 0.001$). All values are represented as mean ± standard deviation ($n = 4$).

Similar to vWF-coated surfaces, P-selectin-coated surfaces had more GPIb-conjugated NPs adhered, compared to control (non-conjugated) NPs (results not shown).

The experimental NP bound densities (markers in Fig. 3) at different shear rates and particle sizes are illustrated via simulation studies as solid lines in Fig. 3. Since the binding of PLGA NPs to coated P-selectin surfaces has been documented (Takalkar et al., 2004), we only presented the binding dynamics of PLGA NPs with vWF-coated surfaces. The bound density at different shear rates was normalized with that at the static condition. It is observed that bound particle density decreases with increased shear rate. This is due to the increasing dislodging force and detachment rates at higher shear rates. At the same shear rate, the adhered particle density is lower for larger particles compared to that for smaller particles. This is attributed to the fact that larger NPs experience larger dislodging forces, resulting in higher detachment rates, thus lower adhered NPs densities. Both simulation and experimental results indicate that nanoparticle adhesion efficacy is higher for smaller particles under lower shear stresses.

We further analyzed the specific interaction of the control and GPIb-conjugated NPs on P-selectin- and vWF-coated surfaces under arterial flow conditions of 15 dyn/cm^2 (Fig. 4). A nearly twofold

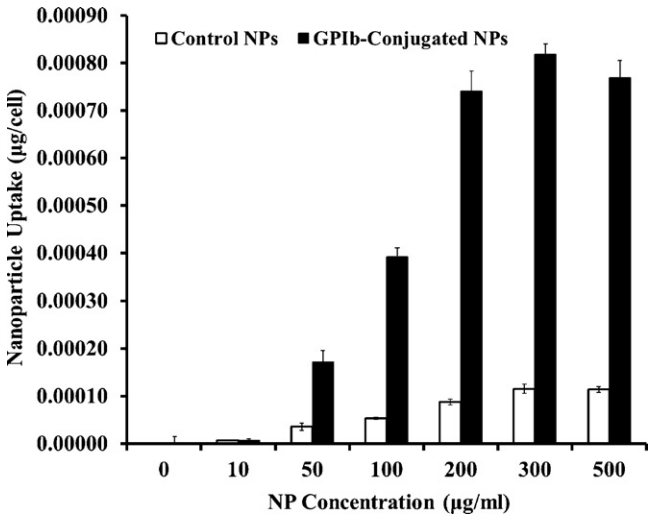

Fig. 2. Effects of NP concentrations on HAEC cellular uptake. Values were obtained after incubating the cells with respective NP suspensions for 1 h.

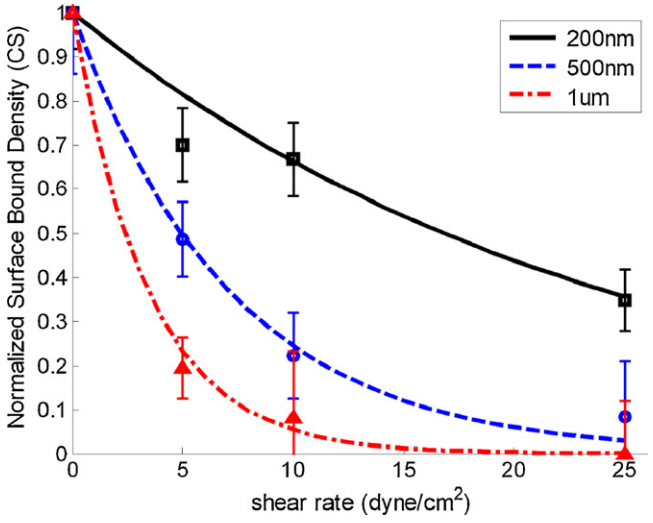

Fig. 3. Normalized nanoparticle bound density at different shear rates and particle sizes. The solid or dotted lines represent the simulated bound density at different shear rates, while the markers represent the experimental bound density data. Lines or continuous curves were plotted from simulation equations as described in Section 2.

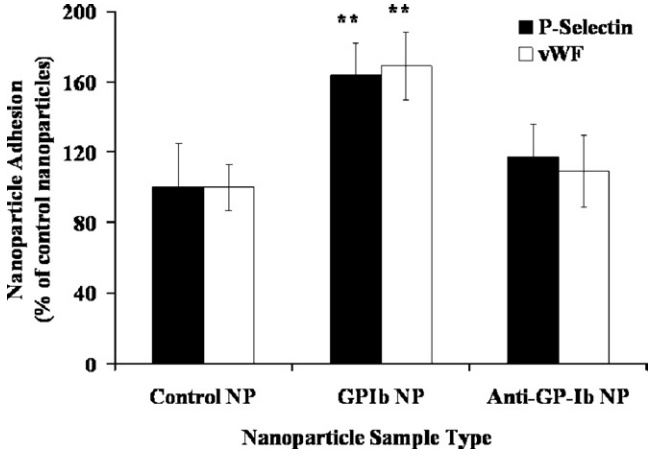

Fig. 4. Adhesion of control and GPIb-conjugated NPs onto P-selectin- and vWF-coated surfaces at a shear stress of 15 dyn/cm^2 for 30 min. Values are represented as mean ± SD ($n = 4$). ** Indicates significant difference compared to the control NP samples ($p < 0.001$).

increase in the adhesion of GPIb-conjugated NPs to P-selectin- and vWF-coated surfaces was observed compared with the control NPs. Using antibodies against GPIb with GPIb-conjugated NPs (anti-GPIb NPs in Fig. 4) or free GPIb peptides for competitive studies (results not shown) also showed that the NP adhesion to P-selectin and vWF-coated surfaces was comparable to those of the control NPs, indicating the importance of the role of GPIb binding to P-selectin and vWF under physiological flow conditions.

Shear regulated cellular uptake and binding studies of control (non-conjugated) and GPIb-conjugated NPs by activated HAECs showed that perfusion of GPIb-conjugated NPs over activated HAECs exhibited a significant cellular uptake, while control NPs displayed lesser cellular uptake (Fig. 5A). In addition, confocal imaging revealed that un-conjugated NPs were mostly detected in extracellular spaces, with minimal NPs within the cells (Fig. 5B). In contrast, NPs conjugated with GPIb showed higher uptake as detected within cells, with a very low concentration of NPs present in extracellular spaces (Fig. 5C).

3.5. *Ex vivo* retention study

As shown in Fig. 6B, GPIb-conjugated NPs adhered more onto the injured arterial wall compared to control NPs (Fig. 6A). In preliminary *ex vivo* adhesion studies using the rat carotid injury model as a proof-of-concept, normalized fluorescent intensities between two nanoparticle groups adhered onto the injured arterial wall showed a significantly higher adhesion (more than twofold retention) of the GPIb-conjugated NPs to the injured vascular wall compared to the control NPs (results not shown).

4. Discussion

The majority of patients with obstructive coronary blockages are usually treated with percutaneous interventions (PCI) such as angioplasty and stenting; however, PCI involves vascular injury caused during inflation of balloons (angioplasty), leading to exuberant smooth muscle cell proliferation and neointimal hyperplasia that results in the re-narrowing of lumen (restenosis) (Brodie et al., 2011). Although immunosuppressive drug-coated metal stents (drug-eluting stents or DES) have reduced restenosis by suppressing neointimal proliferation, they are associated with an increased and prolonged risk of stent thrombosis (clot formation) due to delayed 'healing' or endothelial coverage of exposed stent sturts. Stent thrombosis is associated with over 50% acute mortality, thus patients with DES are treated with potent anti-platelet agents for prolonged durations, and thereby often have severe bleeding complications (Brodie et al., 2011). The use of nanoparticles (NPs) as vehicles for targeted endovascular immunosuppressive drug delivery to address neointimal hyperplasia or restenosis, without the presence of a metal stent as a potential place for clot formation can provide a viable solution to the above problems. Drug-loaded NPs, if delivered to the vessel wall during coronary angioplasty, may suppress neointimal hyperplasia without the need for a permanent endovascular stent. Previously, we have investigated the effects of shear stress on the cellular uptake of nanoparticles by HAECs and proposed the development of endothelial-targeting nanoparticles using polystyrene nanoparticles as a model (Lin et al., 2010). These studies have the shortcoming that nanoparticles made of polystyrene are non-degradable and therefore cannot be used as a real drug delivery carrier. The intent of this research was to further examine our novel strategy of platelet-mimicking nanoparticles for targeted drug delivery to the injured arterial wall and activated HAECs using biodegradable nanoparticles made of the FDA approved material, PLGA.

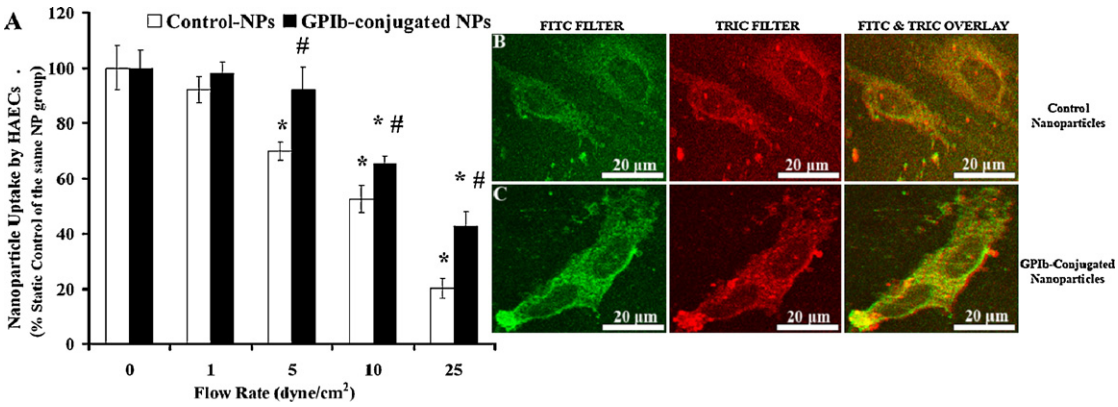

Fig. 5. (A) Adhesion and uptake of control and GPIb-conjugated NPs by activated HAECs under shear stresses via measurement of particles in lysis cell samples. Cells were activated with 25 mM histamine just before flow. Measurements on cell lysis for each sample were made after 30 min of flow. Values represent mean ± SD ($n = 3$). * Indicates the significant differences compared to the same nanoparticle group of static samples ($p < 0.05$). # Denotes the significant difference between GPIb-conjugated NPs and control NPs ($p < 0.05$). (B) Confocal image of ECs taken up of control NPs. (C) Confocal image of ECs taken up of GPIb-conjugated NPs. Fluorescent NPs were imaged using a FITC filter, while plasma membranes were stained with FM® 4-64 FX red membrane dye and imaged using TRIC filter. Images on the far right represent the color overlay of FITC and TRIC filters. Scale bar = 20 μm. (For interpretation of the references to color in this figure legend, the reader is referred to the web version of the article.)

PLGA nanoparticles have been developed previously to provide controlled and sustained drug delivery as PLGA has been approved by the US FDA for the use of drug delivery and diagnostics in cardiovascular disease, cancer, and tissue engineering due to many of its advantages (Jain et al., 2011; Song et al., 2010). One of them is that PLGA degrades slowly *in vivo* and can be used to entrap both water-soluble and water-insoluble therapeutic molecules for sustained drug delivery. As shown in our results, the formulated PLGA NPs produced a sustained drug release for up to 21 days, were stable in different physiological fluids, and demonstrated minimal cytotoxicity in HAECs. The release of the drug dexamethasone from our NPs showed an initial burst release (about 36% in 24 h) owing to drug desorption from the NPs surface, followed by a stable sustained release attributable to both diffusion of the drug and degradation of the PLGA NPs. These results are consistent with the findings reported by other researchers (Cascone et al., 2002; Kim and Martin, 2006; Song et al., 1997). For instance, after 25 days, up to 85% of total DEX release from PLGA NPs was reported by Song et al. (1998), while both Cascone et al. (2002) and Kim and Martin (2006) reported about 90% DEX release from the PLGA NPs over 3 weeks. These results, in addition to our results, indicate that PLGA NPs could be used as drug carriers for targeted and controlled drug delivery, providing a sustained drug release over a time course.

It is well-known that uptake of nanoparticles by targeted cells is affected by various factors including cell types and particle materials. The uptake of PLGA NPs by HAECs was found to be dose- and incubation time-dependent with an optimal dose of 300 μg/ml and an optimal time of 4 h in our studies. These results were similar to the PLGA NP cellular uptake outcomes in previous studies using HUVECs, where uptake saturated at 300 μg/ml (Davda and Labhasetwar, 2002). Contrary to our studies of HAECs, NP uptake saturated after 2 h of exposure in HUVECs. In addition, Caco-2 cells showed a saturated uptake at a dose of 500 μg/ml PLGA particles in 2 h (Desai et al., 1997). Moreover, uptake of polystyrene nanoparticles by HAECs reached saturation at 200 μg/ml within a half hour (Lin et al., 2010), whereas uptake of PLGA nanoparticles by HAECs reached saturation at a higher concentration (300 μg/ml) for a longer time, 4 h, in our studies. Thus our results, in combination with previous findings, suggest that the uptake of drug-loaded nanoparticles by targeted cells needs to be well-characterized to find the optimal particle concentration and incubation time, as this process is dependent not only on cell types but also on particle materials.

The incorporation of specific targeting motifs has been used to enhance the cellular uptake of nanoparticles by targeted cells, and thereby would minimize the drug side effects and enhance drug delivery. In our study, the GPIb-conjugated NPs exhibited an eightfold increase in cellular uptake compared to the control (un-conjugated) NPs. A similar trend in increased uptake of conjugated NPs by cells was observed by Ke et al. (2009) and Xu et al.

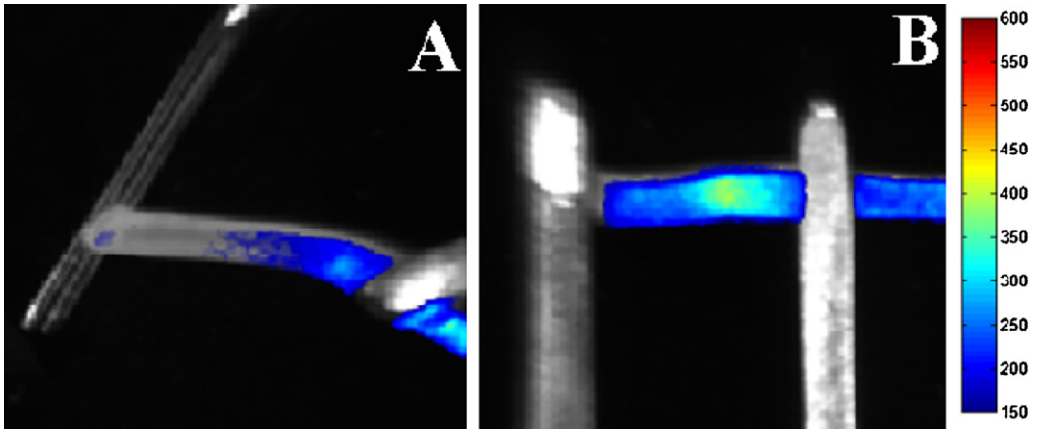

Fig. 6. Images of rat carotid arteries after balloon angioplasty injury and local delivery of (A) control NPs and (B) GPIb-conjugated NPs using the KODAK FX Pro imaging system.

(2009a). Other researchers have also shown that the targeting of drug-laden carriers to the endothelium enhances their availability at the target cells. For instance, Smirnov et al. (1986) found that the conjugation of anti-collagen type I antibodies or fibronectin to liposomes increased their binding to denuded endothelium of arterial segments *in situ*. Muro et al. (2006, 2008) also demonstrated that conjugating polymer nanocarriers with anti-ICAM increased their vascular targeting and internalization by ECs and that the carrier shape influenced vascular targeting and transport into the ECs. In addition, polymer nano-carriers conjugated with anti-PECAM/SA were able to deliver the active encapsulated catalase to the ECs in both cell culture and animal studies (Dziubla et al., 2008). The intracellular localization of NPs as seen by confocal microscopy is due to the endocytosis of the NPs and has been well-documented by other researchers (Qaddoumi et al., 2004; Wiewrodt et al., 2002; Xu et al., 2009b). Results from our and others' studies establish that conjugation of targeting motifs onto nanoparticles would enhance cellular uptake of these drug-loaded nanoparticles by targeted cells, probably through one of the endocytosis pathways.

Other factors, like varying shear stress levels, can also influence the NPs' uptake by endothelial cells. Our studies indicated that increasing the shear stress to 20 dyn/cm^2 decreased the cellular uptake of NPs by HAECs by threefold compared to the static controls. This observation is supported by similar research studies from both our group and others, which have also found that adhesion of NPs on ligand-coated surfaces and activated endothelial cells is inversely related to shear stress levels despite particle materials (Blackwell et al., 2001; Dickerson et al., 2001; Lin et al., 2010). Such decrease in NP adhesion at high shear stress levels and larger particle size is well-explained through the computational model. It is shown that larger dislodging forces under higher shear stresses for bigger particles might wash adhered particles away against adhesion, thus decreasing NP adhesion probability. The computational model also suggests that designing NPs with a higher coating density and a larger contact area/non-spherical shape might improve adhesion efficacy of NPs (Decuzzi and Ferrari, 2006).

To improve the adhesion and targeting capability of NPs to endothelial cells under physiological flow conditions, we designed "platelet-mimicking endothelial-targeting NPs" for better adherence to both P-selectin- and vWF-coated surfaces under physiological flow conditions by imitating the binding of platelets to the injured arterial wall and subendothelium. Other researchers have used leukocyte-imitating particles (Eniola and Hammer, 2005a; Sakhalkar et al., 2003; Zou et al., 2005) and endothelial targeting particles coated with humanized antibodies against E- and P-selectins (Blackwell et al., 2001; Dickerson et al., 2001). Particles (both nano and micro) conjugated with sialyl Lewis^x (sLe^x) (Eniola and Hammer, 2005a,b; Zou et al., 2005), as well as antibodies against P-selectin (Dickerson et al., 2001) and LFA-1 (Eniola and Hammer, 2005b) were also observed to better adhere to P-selectin-, E-selectin- and ICAM-1-coated surfaces, as well as to activated endothelial cells. Just like these studies, our "platelet-mimicking endothelial-targeting NPs", GPIb-conjugated NPs, adhered better to both P-selectin- and vWF-coated surfaces and were taken up more by activated ECs under physiological flow conditions by imitating the binding of platelets to activated ECs, compared to non-conjugated NPs, as shown in our results. This induced adhesion and uptake of GPIb-conjugated NPs might be due to the higher binding strength of platelet ligand–GPIb under high shear stress situations (Andrews et al., 2001; Chen and Lopez, 2005). Preliminary *ex vivo* results also indicate that the GPIb-conjugated NPs have a considerably better retention to the vascular wall on local administration of the NPs in the injured carotid artery of rats. This finding lends support to our hypothesis that modifying the NPs with platelet GPIb would enhance the arterial endothelial retention of drug-loaded agents to treat restenosis.

In summary, this study investigated GPIb-conjugated NPs as mimicking platelet adhesion onto the injured arterial wall for improved binding and targeting to the inflamed endothelial cells and injured arterial wall under fluid shear stress. Conjugation of GPIb to PLGA NPs increased particle adhesion onto targeted surfaces and cellular uptake of these nanoparticles by activated ECs under shear stresses. These GPIb-conjugated NPs also provided a controlled release of the anti-inflammatory drug model. The adhesion efficacy of PLGA NPs of various sizes under physiological shear flow were characterized through a flow chamber study and explained through computer simulations. Our *in vitro* and simulation results suggest that the drug-loaded, GPIb-conjugated PLGA nanoparticles could be used as a targeted and controlled drug delivery system to the site of vascular injury for treatment of cardiovascular diseases. However, the current study did not look into the competitive binding of GPIb-conjugated NPs with platelets, which will be done in the future, along with *in vivo* animal studies. It is also important to note that particles with a large size as our nanoparticles (about 200 nm) would be easily cleared from circulation by the reticuloendothelial system (RES) within a few minutes after administration. To overcome these limitations, local delivery of these nanoparticles to the injured vasculature via infusion catheters (Guzman et al., 1996) or coating of these nanoparticles onto drug-eluting stents to form nanoparticle-eluting stents (Nakano et al., 2009) could be used.

Acknowledgments

The authors would like to acknowledge the assistance provided by members of the Core Imaging Facility at UTSW and the Characterization Center for Materials and Biology at UTA. We also acknowledge the financial support from the NIH grants HL091232 (K.N.) and EB009786 (Y.L.), and NSF grant 0955214 (Y.L.).

References

Andre, P., Hainaud, P., Bal dit Sollier, C., Garfinkel, L.I., Caen, J.P., Drouet, L.O., 1997. Relative involvement of GPIb/IX–vWF axis and GPIIb/IIIa in thrombus growth at high shear rates in the guinea pig. Arterioscler. Thromb. Vasc. Biol. 17, 919–924.

Andrews, R.K., Shen, Y., Gardiner, E.E., Berndt, M.C., 2001. Platelet adhesion receptors and (patho)physiological thrombus formation. Histol. Histopathol. 16, 969–980.

Blackwell, J.E., Dagia, N.M., Dickerson, J.B., Berg, E.L., Goetz, D.J., 2001. Ligand coated nanosphere adhesion to E- and P-selectin under static and flow conditions. Ann. Biomed. Eng. 29, 523–533.

Brodie, B., Pokharel, Y., Fleishman, N., Bensimhon, A., Kissling, G., Hansen, C., Milks, S., Cooper, M., McAlhany, C., Stuckey, T., 2011. Very late stent thrombosis after primary percutaneous coronary intervention with bare-metal and drug-eluting stents for ST-segment elevation myocardial infarction: a 15-year single-center experience. JACC 4, 30–38.

Brown, D.C., Larson, R.S., 2001. Improvements to parallel plate flow chambers to reduce reagent and cellular requirements. BMC Immunol. 2, 9.

Cascone, M.G., Pot, P.M., Lazzeri, L., Zhu, Z., 2002. Release of dexamethasone from PLGA nanoparticles entrapped into dextran/poly(vinyl alcohol) hydrogels. J. Mater. Sci. Mater. Med. 13, 265–269.

Chen, J., Lopez, J.A., 2005. Interactions of platelets with subendothelium and endothelium. Microcirculation 12, 235–246.

Chithrani, B.D., Chan, W.C., 2007. Elucidating the mechanism of cellular uptake and removal of protein-coated gold nanoparticles of different sizes and shapes. Nano Lett. 7, 1542–1550.

Davda, J., Labhasetwar, V., 2002. Characterization of nanoparticle uptake by endothelial cells. Int. J. Pharm. 233, 51–59.

Decuzzi, P., Ferrari, M., 2006. The adhesive strength of non-spherical particles mediated by specific interactions. Biomaterials 27, 5307–5314.

Desai, M.P., Labhasetwar, V., Walter, E., Levy, R.J., Amidon, G.L., 1997. The mechanism of uptake of biodegradable microparticles in Caco-2 cells is size dependent. Pharm. Res. 14, 1568–1573.

Dickerson, J.B., Blackwell, J.E., Ou, J.J., Shinde Patil, V.R., Goetz, D.J., 2001. Limited adhesion of biodegradable microspheres to E- and P-selectin under flow. Biotechnol. Bioeng. 73, 500–509.

Dong, J., Schade, A.J., Romo, G.M., Andrews, R.K., Gao, S., McIntire, L.V., Lopez, J.A., 2000. Novel gain-of-function mutations of platelet glycoprotein IBalpha by valine mutagenesis in the Cys209–Cys248 disulfide loop. Functional analysis under statis and dynamic conditions. J. Biol. Chem. 275, 27663–27670.

Dziubla, T.D., Shuvaev, V.V., Hong, N.K., Hawkins, B.J., Madesh, M., Takano, H., Simone, E., Nakada, M.T., Fisher, A., Albelda, S.M., Muzykantov, V.R., 2008.

Endothelial targeting of semi-permeable polymer nanocarriers for enzyme therapies. Biomaterials 29, 215–227.
Eniola, A.O., Hammer, D.A., 2005a. Characterization of biodegradable drug delivery vehicles with the adhesive properties of leukocytes II: effect of degradation on targeting activity. Biomaterials 26, 661–670.
Eniola, O.A., Hammer, D.A., 2005b. In vitro characterization of leukocyte mimetic for targeting therapeutics to the endothelium using two receptors. Biomaterials 26, 7136–7144.
Giddings, J.C., Banning, A.P., Ralis, H., Lewis, M.J., 1997. Redistribution of von Willebrand factor in porcine carotid arteries after balloon angioplasty. Arterioscler. Thromb. Vasc. Biol. 17, 1872–1878.
Guzman, L.A., Labhasetwar, V., Song, C., Jang, Y., Lincoff, A.M., Levy, R., Topol, E.J., 1996. Local intraluminal infusion of biodegradable polymeric nanoparticles. A novel approach for prolonged drug delivery after balloon angioplasty. Circulation 94, 1441–1448.
Jain, A.K., Das, M., Swarnakar, N.K., Jain, S., 2011. Engineered PLGA nanoparticles: an emerging delivery tool in cancer therapeutics. Crit. Rev. Ther. Drug Carrier Syst. 28, 1–45.
Ke, W., Shao, K., Huang, R., Han, L., Liu, Y., Li, J., Kuang, Y., Ye, L., Lou, J., Jiang, C., 2009. Gene delivery targeted to the brain using an Angiopep-conjugated polyethyleneglycol-modified polyamidoamine dendrimer. Biomaterials 30, 6976–6985.
Kim, D.H., Martin, D.C., 2006. Sustained release of dexamethasone from hydrophilic matrices using PLGA nanoparticles for neural drug delivery. Biomaterials 27, 3031–3037.
Kumar, R.A., Dong, J.F., Thaggard, J.A., Cruz, M.A., Lopez, J.A., McIntire, L.V., 2003. Kinetics of GPIbalpha—vWF—A1 tether bond under flow: effect of GPIbalpha mutations on the association and dissociation rates. Biophys. J. 85, 4099–4109.
Lin, A., Sabnis, A., Kona, S., Nattama, S., Patel, H., Dong, J.F., Nguyen, K.T., 2010. Shear-regulated uptake of nanoparticles by endothelial cells and development of endothelial-targeting nanoparticles. J. Biomed. Mater. Res. A 93, 833–843.
Lutters, B.C., Leeuwenburgh, M.A., Appeldoorn, C.C., Molenaar, T.J., Van Berkel, T.J., Biessen, E.A., 2004. Blocking endothelial adhesion molecules: a potential therapeutic strategy to combat atherogenesis. Curr. Opin. Lipidol. 15, 545–552.
Muro, S., Dziubla, T., Qiu, W., Leferovich, J., Cui, X., Berk, E., Muzykantov, V.R., 2006. Endothelial targeting of high-affinity multivalent polymer nanocarriers directed to intercellular adhesion molecule 1. J. Pharmacol. Exp. Ther. 317, 1161–1169.
Muro, S., Garnacho, C., Champion, J.A., Leferovich, J., Gajewski, C., Schuchman, E.H., Mitragotri, S., Muzykantov, V.R., 2008. Control of endothelial targeting and intracellular delivery of therapeutic enzymes by modulating the size and shape of ICAM-1-targeted carriers. Mol. Ther. 16, 1450–1458.
Nakano, K., Egashira, K., Masuda, S., Funakoshi, K., Zhao, G., Kimura, S., Matoba, T., Sueishi, K., Endo, Y., Kawashima, Y., Hara, K., Tsujimoto, H., Tominaga, R., Sunagawa, K., 2009. Formulation of nanoparticle-eluting stents by a cationic electrodeposition coating technology: efficient nano-drug delivery via bioabsorbable polymeric nanoparticle-eluting stents in porcine coronary arteries. JACC 2, 277–283.
Nguyen, K.T., Eskin, S.G., Patterson, C., Runge, M.S., McIntire, L.V., 2001. Shear stress reduces protease activated receptor-1 expression in human endothelial cells. Ann. Biomed. Eng. 29, 145–152.
Panyam, J., Labhasetwar, V., 2003. Dynamics of endocytosis and exocytosis of poly(D,L-lactide-co-glycolide) nanoparticles in vascular smooth muscle cells. Pharm. Res. 20, 212–220.
Park, T.G., Yoo, H.S., 2006. Dexamethasone nano-aggregates composed of PEG–PLA–PEG triblock copolymers for anti-proliferation of smooth muscle cells. Int. J. Pharm. 326, 169–173.
Petrik, P.V., Law, M.M., Moore, W.S., Colburn, M.D., Quinones-Baldrich, W., Gelabert, H.A., 1998. Dexamethasone and enalapril suppress intimal hyperplasia individually but have no synergistic effect. Ann. Vasc. Surg. 12, 216–220.
Qaddoumi, M.G., Ueda, H., Yang, J., Davda, J., Labhasetwar, V., Lee, V.H., 2004. The characteristics and mechanisms of uptake of PLGA nanoparticles in rabbit conjunctival epithelial cell layers. Pharm. Res. 21, 641–648.
Riper, J.W., Swerlick, R.A., Zhu, C., 1998. Determining force dependence of two-dimensional receptor-ligand binding affinity by centrifugation. Biophys. J. 74, 492–513.
Romo, G.M., Dong, J.F., Schade, A.J., Gardiner, E.E., Kansas, G.S., Li, C.Q., McIntire, L.V., Berndt, M.C., Lopez, J.A., 1999. The glycoprotein Ib–IX–V complex is a platelet counterreceptor for P-selectin. J. Exp. Med. 190, 803–814.
Sakhalkar, H.S., Dalal, M.K., Salem, A.K., Ansari, R., Fu, J., Kiani, M.F., Kurjiaka, D.T., Hanes, J., Shakesheff, K.M., Goetz, D.J., 2003. Leukocyte-inspired biodegradable particles that selectively and avidly adhere to inflamed endothelium in vitro and in vivo. Proc. Natl. Acad. Sci. U.S.A. 100, 15895–15900.
Sakhalkar, H.S., Hanes, J., Fu, J., Benavides, U., Malgor, R., Borruso, C.L., Kohn, L.D., Kurjiaka, D.T., Goetz, D.J., 2005. Enhanced adhesion of ligand-conjugated biodegradable particles to colitic venules. FASEB J. 19, 792–794.
Smirnov, V.N., Domogatsky, S.P., Dolgov, V.V., Hvatov, V.B., Klibanov, A.L., Kotelianski, V.E., Muzykantov, V.R., Repin, V.S., Samokhin, G.P., Shekhonin, B.V., et al., 1986. Carrier-directed targeting of liposomes and erythrocytes to denuded areas of vessel wall. Proc. Natl. Acad. Sci. U.S.A. 83, 6603–6607.
Song, C., Labhasetwar, V., Cui, X., Underwood, T., Levy, R.J., 1998. Arterial uptake of biodegradable nanoparticles for intravascular local drug delivery: results with an acute dog model. J. Control. Release 54, 201–211.
Song, C.X., Labhasetwar, V., Murphy, H., Qu, X., Humphrey, W.R., Shebuski, R.J., Levy, R.J., 1997. Formulation and characterization of biodegradable nanoparticles for intravascular local drug delivery. J. Control. Release 43, 197–212.
Song, X., Zhao, X., Zhou, Y., Li, S., Ma, Q., 2010. Pharmacokinetics and disposition of various drug loaded biodegradable poly(lactide-co-glycolide) (PLGA) nanoparticles. Curr. Drug Metab. 11, 859–869.
Spragg, D.D., Alford, D.R., Greferath, R., Larsen, C.E., Lee, K.D., Gurtner, G.C., Cybulsky, M.I., Tosi, P.F., Nicolau, C., Gimbrone Jr., M.A., 1997. Immunotargeting of liposomes to activated vascular endothelial cells: a strategy for site-selective delivery in the cardiovascular system. Proc. Natl. Acad. Sci. U.S.A. 94, 8795–8800.
Takalkar, A.M., Klibanov, A.L., Rychak, J.J., Lindner, J.R., Ley, K., 2004. Binding and detachment dynamics of microbubbles targeted to P-selectin under controlled shear flow. J. Control. Release 96, 473–482.
Van Put, D.J., Van Hove, C.E., De Meyer, G.R., Wuyts, F., Herman, A.G., Bult, H., 1995. Dexamethasone influences intimal thickening and vascular reactivity in the rabbit collared carotid artery. Eur. J. Pharmacol. 294, 753–761.
Wiewrodt, R., Thomas, A.P., Cipelletti, L., Christofidou-Solomidou, M., Weitz, D.A., Feinstein, S.I., Schaffer, D., Albelda, S.M., Koval, M., Muzykantov, V.R., 2002. Size-dependent intracellular immunotargeting of therapeutic cargoes into endothelial cells. Blood 99, 912–922.
Xu, F., Lu, W., Wu, H., Fan, L., Gao, X., Jiang, X., 2009a. Brain delivery and systemic effect of cationic albumin conjugated PLGA nanoparticles. J. Drug Target. 17, 423–434.
Xu, P., Gullotti, E., Tong, L., Highley, C.B., Errabelli, D.R., Hasan, T., Cheng, J.X., Kohane, D.S., Yeo, Y., 2009b. Intracellular drug delivery by poly(lactic-co-glycolic acid) nanoparticles, revisited. Mol. Pharm. 6, 190–201.
Zou, X., Shinde Patil, V.R., Dagia, N.M., Smith, L.A., Wargo, M.J., Interliggi, K.A., Lloyd, C.M., Tees, D.F., Walcheck, B., Lawrence, M.B., Goetz, D.J., 2005. PSGL-1 derived from human neutrophils is a high-efficiency ligand for endothelium-expressed E-selectin under flow. Am. J. Physiol. Cell Physiol. 289, C415–C424.